journal

J. Am. Ceram. Soc., 79 [1] 177–82 (1996)

# Combustion Synthesis/Dynamic Densification of a $TiB_2$-SiC Composite

Darren A. Hoke,*,† Do Kyung Kim,*,‡ Jerry C. LaSalvia,† and Marc A. Meyers†

Department of Applied Mechanics and Engineering Sciences, University of California, San Diego, La Jolla, California 92093-0411

Department of Ceramic Science and Engineering, Korea Advanced Institute of Science and Technology, Yusong Gu, Taejon 205-701, Korea

**The Ti + 2B exothermic chemical reaction was used in combination with a high-velocity forging step to produce dense $TiB_2$–(20 vol%)SiC composites. Densities in excess of 96% of the theoretical were achieved for both SiC particulate and fiber additions. X-ray diffractometry revealed the products of the reaction to be $TiB_2$ and SiC. The microstructures are composed of spheroidal $TiB_2$ phase, a highly contiguous SiC binder phase, and an apparent eutectic between $TiB_2$ and SiC located at regions of preexisting SiC additions. These microstructural features suggest that SiC underwent a peritectic phase transformation. Thermodynamic analysis predicts that at least 41 vol% SiC addition is needed to prevent the loss of the starting morphologies by the peritectic reaction.**

## I. Introduction

TITANIUM DIBORIDE ($TiB_2$) and $TiB_2$-based composites have received considerable attention in recent years due to their relatively low specific gravities (4.3–4.6 g/cm$^3$), high Vickers hardness values (15–36 GPa), relatively high fracture toughness values ($K_{IC}$ = 6–8 MPa·m$^{1/2}$), good electrical conductivities ($\rho$ = 9–15 $\mu\Omega$·cm at 25°C), and excellent chemical resistance to molten nonferrous metals.[1–3] These characteristics make $TiB_2$ and $TiB_2$-based composites attractive materials for land-based armor, cutting tool, wear resistant, Heroult–Hall cell, and vacuum metallization applications.[1–3]

One major drawback of these materials is their high cost of production. Large bodies of dense $TiB_2$ and $TiB_2$-based composites are produced from presynthesized powders which are densified by sintering, hot pressing, or hot isostatic pressing (HIPing) techniques. Recently, significant progress has been made in the effort to develop reliable, low-cost manufacturing alternatives to the traditional powder metallurgy techniques in general. One such alternative combines combustion synthesis with a densification step.[4–18] Numerous densification methods have been investigated: hot pressing,[10] explosive compaction,[11,12] modified HIP,[13,14] and impact forging.[15–18]

Impact forging has been successfully combined with combustion synthesis to produce dense TiC,[15] TiC–Ni,[16] $TiB_2$,[17] and $Al_2O_3$–$TiB_2$[18] materials. The focus of this investigation is on the synthesis and subsequent densification by the impact forging technique of a $TiB_2$–(20 vol%)SiC composite. SiC was chosen because of its potential as a reinforcing phase in ceramic composites.[19,20] Particulate and fiber morphologies for SiC were used to examine their thermal stability, as well as their effect on the microstructures for these materials.

## II. Experimental Techniques

High-purity powders (>99%) of Ti (Micron Metals, Salt Lake City, UT), crystalline B (Hermann C. Starck, Berlin, Germany), and SiC (CERAC, Milwaukee, WI) were used in this investigation. SiC fibers (Nippon Carbon, Tokyo, Japan) with a purity of approximately 90% were also used. Particle sizes were −325 mesh (~44 μm), while the fiber diameters were 10–14 μm. The powders were dry mixed in polyethylene bottles with a ceramic grinding medium for 24 h under an Ar atmosphere. The composition of the powder mixture corresponds to the chemical equation

$$Ti + 2B + 0.31SiC \rightarrow TiB_2 + 0.31SiC \quad (1)$$

The SiC content corresponds to 20 vol% in the final product. After mixing, green compacts were produced by uniaxially pressing the powders in a stainless steel die, using an axial stress of 55 MPa. The inside diameter of the die was lined with graphite foil (Union Carbide, Electronics Division, Cleveland, OH) as a lubricant. The resulting cylindrical green compacts had a density of approximately 60% of the theoretical value.

Combustion wave velocity and temperature measurements were made on compacts approximately 3.2 cm in diameter and 1.27 cm in height. This was done to quantify the time of completion for the reaction, as well as the cooling rate. The experimental setup for the combustion wave velocity and temperature measurements is shown schematically in Fig. 1. This setup is similar to the one used by Dunmead *et al.*[21] It consists of an enclosed combustion chamber, data acquisition system, and varible transformer. During an experiment, the green compact is placed within an insulated 4.9 cm diameter steel ring to minimize heat losses and simulate the actual assembly used during densification. The insulation consists of $Al_2O_3$–$SiO_2$ refractory board (Zircar Products, Florida, NY). The refractory board is fixed to the inside of the steel ring with $Al_2O_3$ cement. This assembly is vacuum cured for 24 h at 300°C. Two W–Re thermocouples (W–5%Re vs W–26%Re, Omega Engineering, Stamford, CT) are inserted through holes drilled in the side of the assembly such that they are positioned at the top and bottom surfaces of the compact as shown in Fig. 1. These thermocouples are capable of short-time exposures up to 2760°C in an inert atmosphere. The bead size of the thermocouples is approximately 600 μm. During preliminary experiments, the compacts would expand, resulting in a greater than 100% elongation. Because this expansion can damage the thermocouples, the entire steel ring assembly is sandwiched between two graphite plates. Initiation of the reaction is accomplished indirectly by the ignition of 5 g of loose Ti + 2B powder mixture using an electric match placed on top of the compact. An IBM PS/2 model 25 computer interfaced with a Metrabyte DAS-8 (Metrabyte, Taunton, MA) data acquisition board is used to acquire the output from the W–Re thermocouples. The data acquisition system is configured to collect voltage data at a rate of $10^{-2}$ s per point from two separate channels. Before ignition of the loose Ti + 2B powder, the reaction chamber is isolated and

Z. A. Munir—contributing editor

Manuscript No. 194905. Received January 29, 1993; approved April 20, 1995.

Supported by the U.S. Army Research Office under Contract Nos. ARO-DAAL-03-88-K-0194 and ARO-DAAL-03-90G-0204 and by the National Science Foundation under Grant No. CBT8713258. Supported also by the Institute of Mechanics and Materials.

*Member, American Ceramic Society.

†University of California.

‡Korea Advanced Institute of Science and Technology.

pumped down to approximately 20 mm of Hg and then backfilled with Ar to atmospheric pressure. Detailed description of this procedure is reported elsewhere.[22]

Combustion synthesis/dynamic densification experiments were conducted on compacts 9.5 cm in diameter and 2.3 cm in height. The compacts were contained within a specially designed containment assembly during the reaction and densification procedures. The assembly consisted of a tapered stainless steel ring with an $Al_2O_3$–$SiO_2$ refractory insulation board fixed to its inner surface by $Al_2O_3$ cement. This assembly with compact was placed in the workpiece area of the forging machine, remotely ignited using the same procedure as described above, and then densified after a fixed time delay. Details about the forging machine are reported elsewhere.[15] Following densification, the assembly was immediately removed from the forging machine and cooled in vermiculite for 24 h.

Bulk densities of the densified materials were measured by the water immersion technique. Polished surfaces of the as-synthesized and densified materials were observed using optical and scanning electron microscopy (SEM). Substructure of the densified materials was observed using transmission electron microscopy (TEM).

## III. Results and Discussion

### (1) Thermodynamic Considerations

Calculating the adiabatic temperature for the reaction described by Eq. (1) is somewhat complicated by conflicting thermodynamic data concerning SiC.[23–25] According to Ref. 23, SiC undergoes a peritectic reaction (i.e., "melt") at 2818 K, while Ref. 24 indicates that it occurs at 3103 K. The products of the peritectic reaction are C and a homogeneous liquid solution of Si and C. Further difficulty is introduced by the possibility of interactions between SiC and Ti (i.e., formation of carbides and silicides of Ti).[25–27] For calculating the adiabatic temperature, the reaction products are assumed to be given by Eq. (1); consideration of the formation of carbides and silicides of Ti will be discussed later. Two adiabatic temperatures, $T_{ad1}$ and $T_{ad2}$, will be calculated assuming that the peritectic reaction occurs at 2818 and 3103 K, respectively. The heat of reaction at 2818 K is determined by assuming that the products are an ideal solution of C and liquid Si; heat of mixing is assumed negligible. The enthalpy–temperature variation for Eq. (1) is shown in Fig. 2.[23,24,28,29] The adiabatic temperatures $T_{ad1}$ and $T_{ad2}$ are 3105 and 3190 K, respectively. Figure 2 indicates that the SiC addition is predicted to completely decompose into a solution of C and liquid Si regardless of the peritectic reaction temperature. Evidence for the SiC peritectic reaction will be shown later. Figure 3 shows the variation of adiabatic temperature with SiC content assuming the peritectic reaction temperature to be 2818 K. For SiC contents less than 26.6 vol%, complete decomposition is predicted, while for contents greater than 41.4 vol%, no decomposition is predicted. From this analysis, if the peritectic reaction occurs at 2818 K, it is expected that the SiC additions to the Ti-B reaction should "melt."

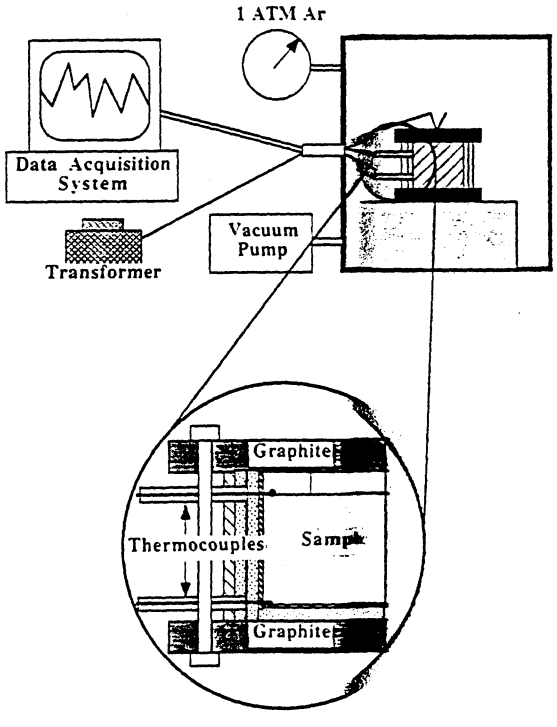


Fig. 1. Experimental configuration for temperature measurement tests illustrating sample confinement and thermocouple placement.

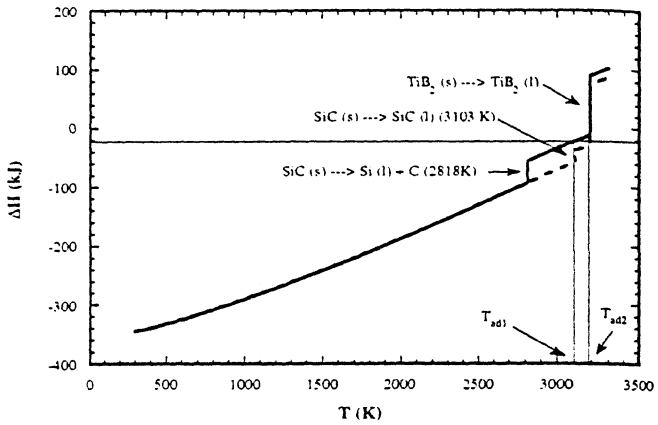


Fig. 2. Adiabatic temperature $T_{ad1}$ and $T_{ad2}$ calculation assuming the peritectic reaction to occur at 2818 and 3103 K, respectively.

### (2) As-Synthesized Materials

Figure 4 shows the X-ray diffraction spectra of both the starting and as-synthesized materials. Before the reaction, the SiC phase is predominately composed of the 6H polytype, with trace amounts of the 3C and 4H polytypes detected. However, after the reaction, only the 6H polytype is detected. It is known that the 6H polytype is thermally more stable than either the 3C or 4H polytypes in the temperature range 2200°–2600°C.[30] This suggests that both the 3C and 4H polytypes were transformed to the 6H polytype.

The resulting highly distended microstructure of the as-synthesized material is shown in Fig. 5. The light areas are the $TiB_2$ phase, while the dark regions are voids. The SiC phase can be distinguished within the $TiB_2$ matrix as gray regions. This highly distended microstructure is due to several factors:[31–33]

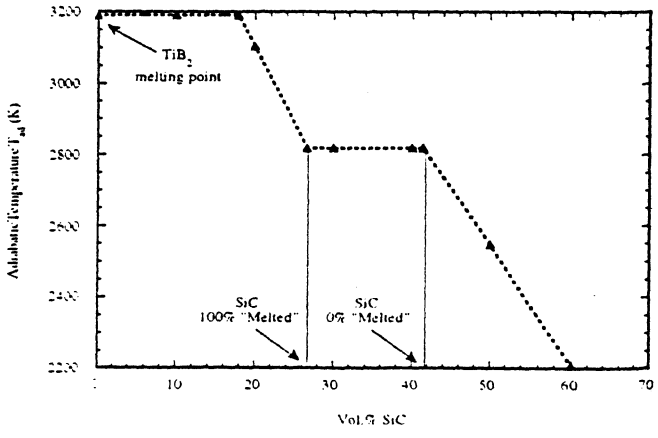


Fig. 3. Variation of adiabatic temperature with volume percent SiC addition assuming the peritectic temperature to be 2818 K.

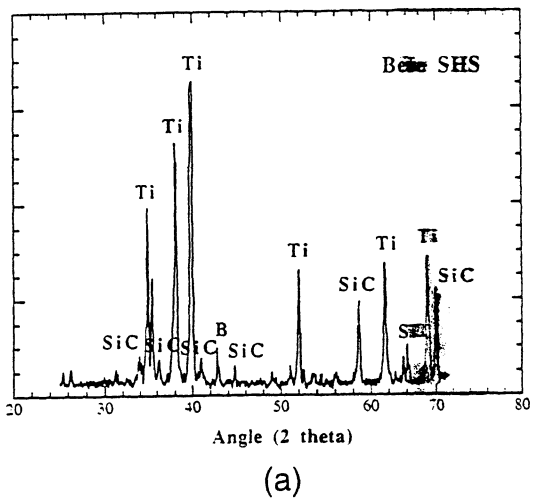


Fig. 4. X-ray diffraction spectra of (a) unreacted powders, and (b) reaction-synthesized composite illustrating complete conversion to $TiB_2$–SiC.

(1) initial porosity, (2) lower specific volume of the products compared to the reactants, (3) capillary flow of least refractory constituent, and (4) expulsion of volatilized impurities.

The as-synthesized microstructures for the particulate and fiber morphologies of SiC are qualitatively different, and this is believed to be due to differences in purity. Figure 6 shows optical micrographs of polished and etched cross sections for both the particulate and fiber morphologies. As can be seen in Fig. 6(a), the resulting microstructure for particulate SiC is characterized by spheroidal $TiB_2$ particles (indicated by arrow). SiC binder phase between the $TiB_2$ particles and an unidentified eutectic occurring in regions of apparent preexisting SiC particles. The SiC binder phase between the $TiB_2$ particles is evidence that the SiC phase underwent the peritectic reaction and later resolidified. Further evidence that the SiC particles underwent the peritectic reaction is seen by the presence of the eutectic. To the author's knowledge, no eutectic microstructure between SiC and $TiB_2$ has been observed. However, this does not rule out its existence, since both Si–C and Ti–B binary phase diagrams exhibit eutectic points.[34,35] Eutectic microstructures have been observed between various borides and carbides.[36,37] Another possible explanation for the peritectic is that it is the result of reactions between Ti and SiC. Reactions between Ti and SiC and their products are well known.[38] The products of the reactions include carbides (TiC, $Ti_3SiC_2$ and $Ti_5Si_3C_x$) and silicides (TiSi, $TiSi_2$, and $Ti_5Si_3$). The formation of these phases is not surprising, since they are thermodynamically favored. Furthermore, the formation of a eutectic is possible,

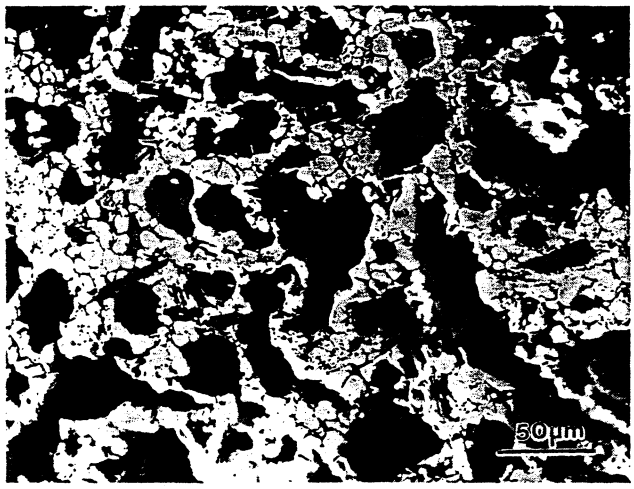


Fig. 5. Electron micrograph of reaction-synthesized $TiB_2$–20 vol% SiC composite.

since both the Ti–C and Ti–Si binary phase diagrams exhibit eutectic points.[38,39] The following chemical reactions and their enthalpies of formation (per mole of Ti) resulting in the formation of TiC and Ti silicides[4] are possible:

$$Ti + 2B \rightarrow TiB_2 \qquad \Delta H_f = -323.8 \text{ kJ/mol} \tag{2}$$

$$Ti + 0.5SiC \rightarrow 0.5(TiC + TiSi) \qquad \Delta H_f = -124.1 \text{ kJ/mol} \tag{3}$$

$$Ti + 0.67SiC \rightarrow 0.67TiC + 0.33TiSi_2 \qquad \Delta H_f = -122.0 \text{ kJ/mol} \tag{4}$$

$$Ti + 0.375SiC \rightarrow 0.375TiC + 0.125Ti_5Si_3 \qquad \Delta H_f = -115.9 \text{ kJ/mol} \tag{5}$$

$$Ti + SiC \rightarrow TiC + Si \qquad \Delta H_f = -115.6 \text{ kJ/mol} \tag{6}$$

Thermodynamically, reaction (2) is the most favorable; however, reactions (3)–(6) are also exothermic and may therefore occur, especially at contact regions between Ti and SiC. However, given that reaction (2) is much more exothermic (per mole of Ti) compared to reactions (3)–(6), it is expected that $TiB_2$ and SiC will be the main reaction products if there is no kinetic inhibition (e.g., melting). One characteristic of the combustion synthesis process is the formation of a liquid phase, or "melt," which not only accelerates the reaction between components, but also enhances the microstructural and chemical homogeneity of the resulting products.[40] For the particle sizes used in this investigation, kinetic inhibition due to melting and subsequent capillary flow is not expected.[41] The X-ray diffraction spectrum shown in Fig. 4(b) shows only $TiB_2$ and SiC peaks and therefore supports the above thermodynamic discussion. The dominant mechanisms involved in the formation of the resulting microstructure are not known; however, based upon previous studies on the micromechanisms of combustion synthesis, a possible model can be described.[42] Assuming that very little reaction product is formed within the heat-affected portion of the combustion wave, the first major physical change will be the melting and capillary spreading of Ti or Ti–B eutectic.[42] Interfacial reactions between Ti and B, as well as Ti and SiC will occur. As a result, both TiC and Ti silicides will form. However, the formation of Ti silicides also results in the enrichment of the existing melt with Si, because their melting points are much lower than the adiabatic temperature (e.g., $TiSi_2$ and $Ti_5Si_3$, 1773 and 2403 K, respectively.[39]) If TiC precipitates from the melt, it will be converted to $TiB_2$ plus free C, since the melt contains some B in solution and $TiB_2$ is more stable than TiC. This free C then reacts with the Si in the melt to form SiC. As a result, only $TiB_2$ and SiC are formed.

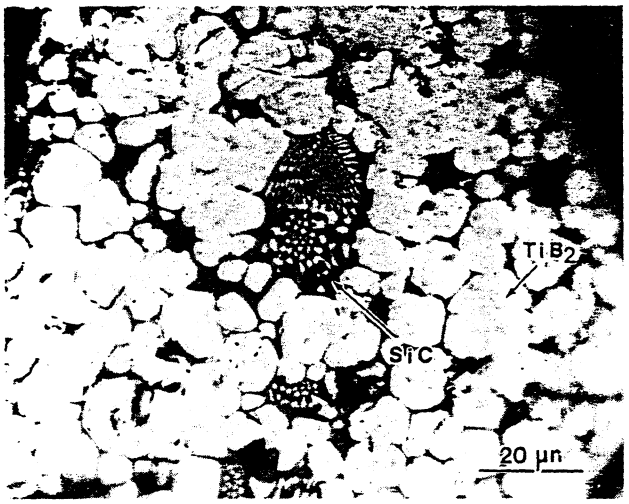


(a)

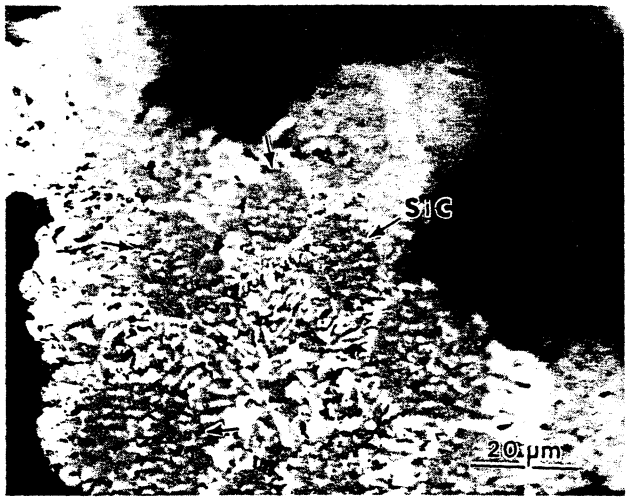


(b)

Fig. 6. Optical micrographs of reaction-synthesized $TiB_2$–20 vol% SiC composites (a) particulate and (b) fiber reinforced. Lighter phases are $TiB_2$, darker phases are SiC, and black areas are porosity.

Figure 6(b) shows the resulting as-synthesized microstructure using the SiC fibers. As can be seen, the eutectic microstructure also exists between the SiC fibers, as well as within the preexisting fiber regions. According to Ref. 43, the major impurities in the SiC fibers (i.e., Nicalon) are free C and $SiO_2$. These impurities are uniformly dispersed within the fiber. Evidently, during the reaction, the $SiO_2$ impurities melt and flow into the region surrounding the fibers. SiC is expected to form by the reaction of the $SiO_2$ melt with the free C, since this reaction is thermodynamically favorable. Again, the main reaction products are $TiB_2$ and SiC.

### *(3) Combustion Synthesized/Dynamically Densified Materials*

As can be seen in Fig. 5, the as-synthesized materials are highly porous and thus require densification. Experimental measurement of the temperature history during and after the reactions is useful for the establishment of a time window for densification, as well as the combustion wave velocity and temperature. A typical temperature history profile for the as-synthesized material is shown in Fig. 7. Data from the top and bottom thermocouples are represented by the solid and dashed lines, respectively. As can be seen, the profiles exhibit a

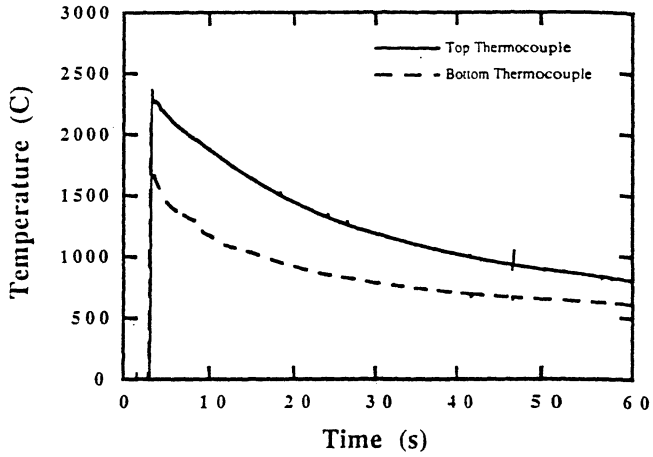


Fig. 7. Experimentally determined temperature vs time profiles for reaction-synthesized $TiB_2$–20 vol% SiC.

sharp rise, indicating the arrival of the combustion front, followed by gradual cooling. The average combustion wave velocity is approximately 8.4 cm/s. The maximum temperature is approximately 2673 K. Given the size of the thermocouple bead, as well as other reasons,[44] an error in the maximum temperature of several hundred degrees is likely.[45] Surface temperatures drop below the $TiB_2$ ductile-to-brittle transition temperature, ~2073 K,[46] within 10 to 15 s after ignition. Thus, assuming that the densification behavior is dependent only on the physicomechanical state of $TiB_2$, the time window for successful densification is 5–15 s after ignition.

The measured bulk densities of the densified materials is shown in Fig. 8 as a function of specific energy. The specific energy is defined as the energy stored in the Dynapak forging machine divided by the mass of the compact (changes in specific energy were accomplished by varying the mass of the compacts, 200 to 300 g). As can be seen, the bulk densities ranged from about 86% to 96% of the theoretical density (i.e., 4.29 g/cm$^3$, as calculated from the rule of mixtures). The densification behavior of the $TiB_2$–SiC material (independent of SiC addition morphology) is similar to that of combustion synthesized/dynamically densified $TiB_2$ and $TiB_2$–1.5 wt% Ni materials obtained earlier.[17]

The highest density (>96% of theoretical density) was obtained at a specific energy of approximately 0.076 J/kg. Increasing the specific energy beyond this value actually resulted in a decrease in density. The decrease in density is thought to be mainly due to the loss of specimen containment during densification. However, the as-synthesized material

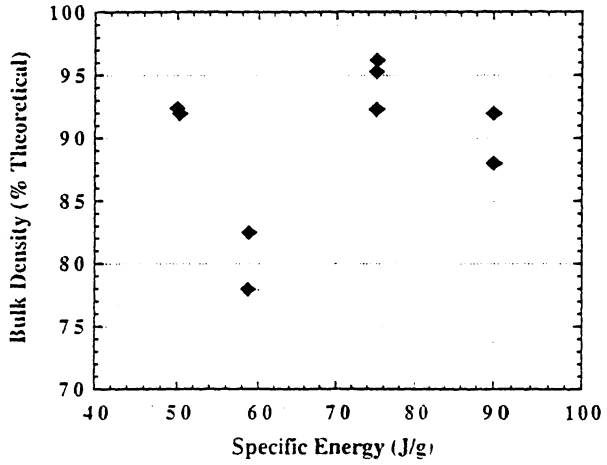


Fig. 8. Bulk density vs specific energy for SHS/DC $TiB_2$–20 vol% SiC.

integrity is also believed to affect the resulting density (for a fixed specific energy). Material integrity was generally maintained after synthesis; however, the volume of the compact increased substantially by expansion perpendicular to the combustion wave propagation direction, thereby creating an open skeletal structure. While this expansion reduced the heat loss due to heat conduction, it increased the heat losses due to both convection and radiation. At such high temperatures, radiative heat loss is dominant. The material cools more rapidly and, as a consequence, its strength increases. Thus, for a fixed deformation energy, assuming the material to be perfectly plastic with a temperature dependent flow stress, the resulting density will be lower. Current efforts are aimed at minimizing this expansion through constraint and the addition of inert diluents.

As mentioned above, the main reason that increasing the specific energy did not result in an increase in density was the loss of specimen containment. This problem was experienced in previous work on TiC[15] and $TiB_2$.[17] During densification, the material deforms in both the axial and radial directions. This radial deformation is allowed, due to a small gap between the compact and the refractory insulation. However, after this gap has been eliminated by the radial deformation, the stress state (i.e., hydrostatic and deviatoric magnitudes) within the compact increases, resulting in a corresponding increase in the densification rate. Eventually, the normal stress at the interface between the compact and the insulation reaches a level that exceeds its strength, resulting in the partial collapse of the insulation (i.e., permanent deformation). This creates a small gap between the insulation and the hammer, enabling part of the compact to extrude out. The failure of the insulation and subsequent loss of containment results in a decrease in the stress levels within the compact. As a consequence, the densification rate is reduced to zero, and no further increase in density is obtained. An alternative method of confinement has been investigated.[16] This method consists of completely surrounding the compact with a granular medium which, during densification, transmits and redistributes the applied load such that the compact exists in a state of quasi-isostatic stress.[47] The use of the granular pressure transmitting medium for the densification of combustion-synthesized materials was pioneered by researchers in the former Soviet Union[48] and in the United States.[49]

Scanning electron micrographs of the dynamically densified materials are shown in Fig. 9. As can be seen in Fig. 9(a), the microstructures are the same as those observed for the as-synthesized materials, with the exception of the reduced porosity. In addition, the lamellar features were much finer than those of the as-synthesized materials and were not visible under optical examination. This is believed to be the result of a higher initial cooling rate caused by the densification process. A close-up of a region consisting of a mixture of SiC and $TiB_2$ is shown in Fig. 9(b). Small $TiB_2$ grains (on the order of 3–4 μm) are evident within this region (marked by arrow A). Figure 10 is a transmission electron micrograph showing the substructure of these materials. The faceted SiC grains are submicrometer in size and show evidence of plastic deformation (high density of dislocations and twinning) as a consequence of the densification step. Excellent wetting behavior of the SiC "melt" on the $TiB_2$ particles is illustrated in the backscattered electron micrograph shown in Fig. 11.

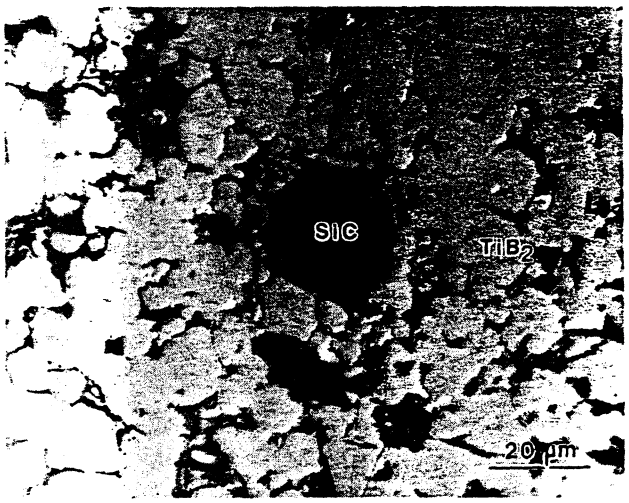


(a)

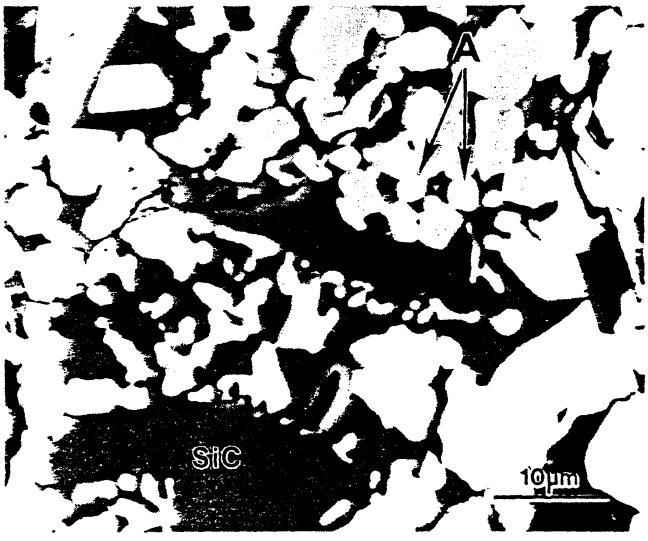


(b)

Fig. 9. Microstructure of SHS/DC $TiB_2$–20 vol% SiC (a) low magnificaton, and (b) high magnification, illustrating melting of SiC particles and formation of small (3–4 μm) $TiB_2$ grains (arrow A).

## IV. Conclusions

It has been demonstrated that dense $TiB_2$–SiC composites can be produced utilizing the Ti − 2B combustion synthesis reaction with a dynamic densification step. Densities in excess of 96% of the theoretical density were obtained. Microstructures consisted of spheroidal $TiB_2$ particles, a nearly continuous SiC binder, and an unidentified eutectic (possibly $TiB_2$–SiC) located at regions corresponding to preexisting SiC particles or


Fig. 10. Transmission electron micrograph of SHS/DC $TiB_2$–20 vol% SiC.

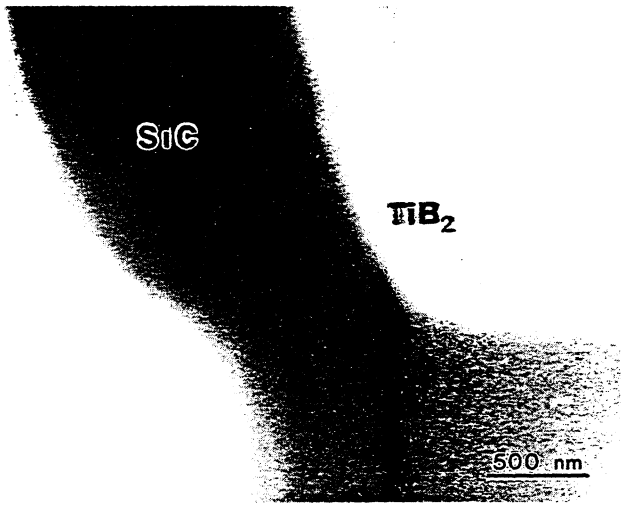


**Fig. 11.** High-magnification backscattered electron image of SHS/DC $TiB_2$–20 vol% SiC illustrating the interfacial region between $TiB_2$ and SiC.

fibers. The regions near the preexisting SiC additions were qualitatively different for the particulate and fiber morphologies. This difference is believed to be due to the difference in purity of the starting materials. These features suggest that the SiC particles "melted." Thermodynamic analysis predicts that 41 vol% dilution with SiC additions is needed to lower the adiabatic temperature below the peritectic reaction temperature and therefore prevent the loss of their starting morphologies.

**Acknowledgments:** Professor K. S. Vecchio provided the IBM PC and software for the combustion wave temperature measurements. Mr. R. Kanemoto was instrumental in much of this investigation.

## References

[1]W. J. Lackey, D. P. Stinton, G. A. Cerny, P. C. Schaffhauser, and L. L. Fehrenbacher. *Adv. Ceram. Mater.*, **2** [1] 24–30 (1987).
[2]Technical Information, Titanium Diboride Powder, Grades HCT–20, 30, 40, F, S, SB, and 30D. Union Carbide Advanced Ceramics, Cleveland, OH.
[3]Technical Information, Manufactured Technical Ceramics. CERCOM, Inc., Vista, CA.
[4]N. P. Novikov, I. P. Borovinskaya, and A. G. Merzhanov, "Thermodynamic Analysis of Self-Propagating High-Temperature Synthesis Reactions"; in *Combustion Processes in Chemical Technology and Metallurgy (Engl. Transl.)*. Edited by A. G. Merzhanov. Chernogolovka, USSR, 1975.
[5]Z. A. Munir, "Synthesis of High Temperature Materials for Self-Propagating Combustion Methods," *Am. Ceram. Soc. Bull.*, **67** [2] 342–49 (1988).
[6]A. G. Merzhanov, "Self-Propagating High-Temperature Synthesis: Twenty Years of Search and Findings"; pp. 1–53 in *Combustion and Plasma Synthesis of High Temperature Materials*. Edited by Z. A. Munir and J. B. Holt. VCH Publishers, New York, 1990.
[7]J. F. Crider, "Self-Propagating High Temperature Synthesis—A Soviet Method for Producing Ceramic Materials," *Ceram. Eng. Sci. Proc.*, **3**, 519–28 (1982).
[8]Z. A. Munir and U. Anselmi-Tamburini, "Self-Propagating Exothermic Reactions: The Synthesis of High-Temperature Materials by Combustion," *Mater. Sci. Rep.*, **3**, 277–365 (1989).
[9]A. N. Pityulin, Yu. V. Bogatov, and A. S. Rogachev, "Gradient Hard Alloys," *Int. J. Self-Propag. High-Temp. Synth.*, **1** [1] 111–17 (1992).
[10]S. D. Dunmead, Z. A. Munir, J. B. Holt, and D. Kingman, "Simultaneous Synthesis and Densification of TiC/Ni–Al Composites," *J. Mater. Sci.*, **26**, 2410–16 (1991).
[11]A. Niiler, L. J. Kecskes, T. Kottke, P. H. Netherwood Jr., and R. F. Benck, "Explosive Consolidation of Combustion Synthesized Ceramics: TiC and $TiB_2$," Ballistics Reseach Laboratory Report BRL-MR-2951, Aberdeen Proving Ground, MD. December 1988.
[12]B. H. Rabin, G. E. Korth, and R. L. Williams, "Fabrication of Titanium Carbide–Alumina Composites by Combustion Synthesis and Subsequent Dynamic Consolidation," *J. Am. Ceram. Soc.*, **73** [2] 156–57 (1990).
[13]Y. Miyamoto, M. Koizumi, and O. Yamada, "High-Pressure Self-Combustion Sintering for Ceramics," *J. Am. Ceram. Soc.*, **67** [11] C-224 (1984).
[14]O. Yamada, Y. Miyamoto, and M. Koizumi, "High-Pressure Self-Combustion Sintering of Titanium Carbide," *J. Am. Ceram. Soc.*, **70** [9] C-206–C-208 (1987).
[15]J. C. LaSalvia, L. W. Meyer, and M. A. Meyers, "Densification of Reaction-Synthesized Titanium Carbide by High-Velocity Forging," *J. Am. Ceram. Soc.*, **75** [3] 592–602 (1992).
[16]J. C. LaSalvia, M. A. Meyers, and D. K. Kim, "Combustion Synthesis/Dynamic Densification of TiC–Ni Cermets," *J. Mater. Synth. Process.*, **2** [4] 255–74 (1994).
[17]D. A. Hoke, M. A. Meyers, L. W. Meyer, and G. T. Gray III, "Reaction Synthesis/Dynamic Compaction of Titanium Diboride," *Metall. Trans. A*, **23A**, 77–86 (1992).
[18]M. A. Meyers, J. C. LaSalvia, D. A. Hoke, J. M. Jamet, and D. K. Kim, "Combustion Synthesis/Densification of Ceramics and Ceramic Composites"; pp. 43–57 in *International Conference on Advanced Synthesis of Engineered Structural Materials*. ASM International, Materials Park, OH, 1993.
[19]N. D. Corbin, G. A. Rossetti, and S. D. Hartline, "Microstructure/Property Relationships for SiC Filament-Reinforced RBSN," *Ceram. Eng. Sci. Proc.*, **7** [7–8] 958–68 (1986).
[20]Y. M. Chiang, J. S. Haggerty, R. P. Messner, and C. Demetry, "Reaction-Based Processing Methods for Ceramic-Matrix Composites," *Am. Ceram. Soc. Bull.*, **68** [2] 420–28 (1989).
[21]S. D. Dunmead, Z. A. Munir, and J. B. Holt, "Temperature Profile Analysis in Combustion Synthesis: II, Experimental Observations," *J. Am. Ceram. Soc.*, **75** [1] 180–88 (1992).
[22]D. A. Hoke and M. A. Meyers, "Consolidation of Combustion Synthesized Titanium Diboride-Based Materials," *J. Am. Ceram. Soc.*, in press.
[23]O. Knacke, O. Kubaschewski, and H. Hesselman (Eds.), *Thermochemical Properties of Inorganic Substances: II*, 2nd ed.; pp. 1848–49. Springer-Verlag, New York, 1991.
[24]L. V. Gurvich, I. V. Veyts, C. B. Alcock, and V. S. Iorish (Eds.), *Thermodynamic Properties of Individual Substances*, Vol. 2, Part 2; p. 263. Hemisphere Publishing Company, New York, 1991.
[25]A. L. Borisova, Yu. S. Borisov, B. A. Polyanin, L. K. Shvedova, V. R. Kalinovskii, and I. N. Gorbatov, "The Reaction in Ti–SiC Composite Powders and the Properties of the Sprayed Coatings," *Sov. Powder Metall. Met. Ceram. (Engl. Transl.)*, **274** [10] 769–73 (1985).
[26]M. Backhaus-Ricoult, "Solid State Reactions between Silicon Carbide and Various Transition Metals," *Ber. Bunsen-Ges. Phys. Chem.*, **93**, 1277–81 (1989).
[27]G. Das, "A Study of the Reaction Zone in an SiC Fiber-Reinforced Titanium Alloy Composite," *Metall. Trans. A*, **21A**, 1571–78 (1990).
[28]M. W. Chase Jr., C. A. Davies, J. R. Downey Jr., D. J. Frurip, R. A. McDonald, and A. N. Syverud, *JANAF Thermochemical Tables*, 3rd ed., Part I, Al-Co. *J. Phys. Chem. Ref. Data*, Suppl. 1, **14**, 535 (1985).
[29]I. Barin, *Thermochemical Data of Pure Substances*, Part II; pp. 19, 1334. VCH Publishers, New York, 1989.
[30]Y. Inomata, "Crystal Chemistry of Silicon Carbide"; pp. 1–11 in *Silicon Carbide Ceramics*, Vol. 1. Edited by S. Somiya and Y. Inomata. Elsevier Applied Science, New York, 1991.
[31]R. W. Rice and W. J. McDonough, "Intrinsic Volume Changes of Self-Propagating Synthesis," *J. Am. Ceram. Soc.*, **68** [5] C-122–C-123 (1985).
[32]V. M. Shkiro and I. P. Borovinskaya, "Capillary Flow of Liquid Metal during Combustion of Titanium Mixtures with Carbon," *Combust. Explos. Shock Waves (Engl. Transl.)*, **12** [6] 828–31 (1976).
[33]A. K. Filonenko and V. I. Vershinnikov, "Gas Emission from Impurities in Gasless Burning of Mixtures of Transition Metals with Boron," *Sov. J. Chem. Phys.*, **3** [3] 675–82 (1985).
[34]T. B. Massalski (Ed.), *Binary Alloy Phase Diagrams*, Vol. 1; pp. 882–83. American Society for Metals, Metals Park, OH, 1986.
[35]See Ref. 34, pp. 544–48.
[36]V. S. Stubican and R. C. Bradt, "Eutectic Solidification in Ceramic Systems," *Ann. Rev. Mater. Sci.*, **11**, 267–97 (1981).
[37]E. A. Levashov, Yu. V. Bogatov, A. S. Rogachev, A. N. Pityulin, I. P. Borovinskaya, and A. G. Merzhanov, "Specific Features of Structure Formation of Synthetic Hard Tool Materials in the SHS Compacting Process," *J. Eng. Phys. Thermophys.*, **63** [5] 1091–105 (1992).
[38]See Ref. 34, pp. 888–91.
[39]See Ref. 34, Vol. 3, pp. 3367–71.
[40]A. G. Merzhanov and A. S. Rogachev, "Structural Macrokinetics of SHS Processes," *Pure Appl. Chem.*, **64** [7] 941–53 (1992).
[41]A. I. Kirdyashkin, Yu. M. Maksimov, and A. G. Merzhanov, "Effects of Capillary Flow on Combustion in a Gas-Free System," *Combust. Explos. Shock Waves*, **17** [6] 591–95 (1982).
[42]Y. M. Maksimov, O. K. Lepakova, and L. G. Raskolenko, "Combustion Mechanism of a Titanium-Boron System with the Use of Quenching of the Reaction Front," *Combust. Explos. Shock Waves*, **24**, 43–48 (1988).
[43]T. Ishikawa, "Silicon Carbide Continuous Fiber (Nicalon)"; pp. 81–98 in *Silicon Carbide Ceramics*, Vol. 2. Edited by S. Somiya and Y. Inomata. Elsevier Applied Science, New York, 1991.
[44]J. C. LaSalvia, "An Investigation into the Synthesis and Processing of Dense Titanium Carbide-Nickel-Molybdenum Based Cermets Utilizing Combustion Synthesis with Impact Forging"; Ph.D. Dissertation. University of California, San Diego, 1994.
[45]T. Boddington, P. G. Laye, J. R. G. Pude, and J. Tipping, "Temperature Profile Analysis of Pyrotechnic Systems," *Combust. Flame*, **47**, 235–54 (1982).
[46]J. R. Ramberg and W. S. Williams, "High Temperature Deformation of Titanium Diboride," *J. Mater. Sci.*, **22**, 1815–26 (1987).
[47]V. M. Gorokhov, E. V. Zvonarev, and M. S. Koval'chenko, "Densification Kinetics of Porous Materials in Hot Pressing under Quasi-Isostatic Conditions. I. Derivation of a Kinetic Densification Equation," *Sov. Powder Metall. Met. Ceram. (Engl. Transl.)*, **90** [10] 756–60 (1978).
[48]*J. Eng. Physics Thermophys.*, **63** [5] (1992); *Int. J. Combust. Synth.*, **1–3**, (1992–94).
[49]R. V. Raman, "Advances in Full Density Consolidation of Engineered Materials"; presented at the 1992 Powder Metallurgy World Congress, San Francisco, CA, June 21–26, 1992. □